Electron Transfer Kinetics in Photosynthetic Reaction Centers Embedded in Trehalose Glasses: Trapping of Conformational Substates at Room Temperature

Gerardo Palazzo,* Antonia Mallardi,† Alejandro Hochkoeppler,‡ Lorenzo Cordone,§ and Giovanni Venturoli¶

*Dipartimento di Chimica, Università di Bari, 70126 Bari and DISTAAM, Università del Molise, 86100 Campobasso, Italy; †Istituto per i Processi Chimico-Fisici, CNR (former CS-CFILM), Bari, Italy; ‡Dipartimento di Chimica Industriale e dei Materiali, Università di Bologna, 40136 Bologna, Italy; §Dipartimento di Scienze Fisiche ed Astronomiche and INFM, 90123 Palermo, Italy; and ¶Laboratorio di Biochimica e Biofisica, Dipartimento di Biologia, Università di Bologna, 40126 Bologna, Italy

ABSTRACT We report on room temperature electron transfer in the reaction center (RC) complex purified from *Rhodobacter sphaeroides*. The protein was embedded in trehalose-water systems of different trehalose/water ratios. This enabled us to get new insights on the relationship between RC conformational dynamics and long-range electron transfer. In particular, we measured the kinetics of electron transfer from the primary reduced quinone acceptor (Q_A^-) to the primary photo oxidized donor (P^+), by time-resolved absorption spectroscopy, as a function of the matrix composition. The composition was evaluated either by weighing (liquid samples) or by near infrared spectroscopy (highly viscous or solid glasses). Deconvolution of the observed, nonexponential kinetics required a continuous spectrum of rate constants. The average rate constant ($\langle k \rangle$ = 8.7 s^{-1} in a 28% (w/w) trehalose solution) increases smoothly by increasing the trehalose/water ratio. In solid glasses, at trehalose/water ratios ≥97%, an abrupt $\langle k \rangle$ increase is observed ($\langle k \rangle$ = 26.6 s^{-1} in the driest solid sample). A dramatic broadening of the rate distribution function parallels the above sudden $\langle k \rangle$ increase. Both effects fully revert upon rehydration of the glass. We compared the kinetics observed at room temperature in extensively dried water-trehalose matrices with the ones measured in glycerol-water mixtures at cryogenic temperatures and conclude that, in solid trehalose-water glasses, the thermal fluctuations among conformational substates are inhibited. This was inferred from the large broadening of the rate constant distribution for electron transfer obtained in solid glasses, which was due to the free energy distribution barriers having become quasi static. Accordingly, the RC relaxation from dark-adapted to light-adapted conformation, which follows primary charge separation at room temperature, is progressively hindered over the time scale of $P^+Q_A^-$ charge recombination, upon decreasing the water content. In solid trehalose-water glasses the electron transfer process resulted much more affected than in RC dried in the absence of sugar. This indicated a larger hindering of the internal dynamics in trehalose-coated RC, notwithstanding the larger amount of residual water present in comparison with samples dried in the absence of sugar.

INTRODUCTION

Proteins assume an extremely large number of conformations (conformational substates), which reflect their complex energy landscape. At physiological temperature, suitable nonharmonic contributions to internal motions (often called protein-specific motions) enable the protein to sample the above landscape by continuous jumps among the different conformations. This conformational flexibility is intimately connected to protein reactivity (see e.g., Frauenfelder et al., 1988, 1991; Frauenfelder and Wolynes, 1994, Frauenfelder and McMahon, 1998). Since the pioneering work of Austin et al. (1975), most of the information on the interplay between protein dynamics and reactivity has come from kinetic studies of ligand binding to heme proteins as a function of temperature. At cryogenic temperatures protein-specific motions are slowed down on the time scale of the studied reaction, and a continuous spectrum of reaction rates is usually observed (inhomogeneous reaction kinetics). This spectrum reflects the heterogeneity of the ensemble of the protein molecules frozen in different conformational substates, each characterized by a different reaction rate. In recent years inhomogeneous reaction kinetics have been detected both in carboxy-myoglobin (Hagen et al., 1995, 1996) and in carboxy-hemoglobin (Gottfried et al., 1996) embedded in room temperature glasses. The freezing of conformational substates can be achieved at room temperature by embedding the protein within a dry trehalose matrix. In this environment protein-specific motions appeared to be severely hindered as shown by Mössbauer and optical absorption spectroscopy, neutron scattering, and molecular dynamics simulation (Cordone et al., 1998, 1999; Cottone et al., 2001). Moreover it has been shown that in carboxy-myoglobin embedded in a trehalose glass the thermal interconversion among conformational A substates (Makinen et al., 1979; Vojtechovsky et al., 1999) is progressively hindered by decreasing the sample water content (Librizzi et al., 1999 and work in progress). In particular, such interconversion was barely detectable in extremely dry samples, which contained only traces of residual, tightly bound water molecules.

Trehalose is a disaccharide found in large amounts in organisms that can survive conditions of extreme dehydra-

Submitted August 14, 2001 and accepted for publication October 24, 2001.

Address reprint requests to Lorenzo Cordone, Dipartimento di Scienze Fisiche ed Astronomiche, Via Archirafi 36, I-90123 Palermo, Italy. Tel.: 39-091-6234215; Fax: 39-091-6162461; E-mail: cordone@fisica.unipa.it.

0006-3495/02/02/558/11 $2.00

tion and high temperatures (>60°C) remaining in the absence of metabolic processes (anydrobiosis) for several years. Among saccharides, trehalose has the highest glass-transition temperature (Green and Angell, 1989) and has been found to be the most active for the preservation of biostructures (see e.g., Leslie et al., 1995; Uritani et al., 1995; Crowe et al., 1996).

In the present work, the reduction of protein dynamics by incorporation into a trehalose glassy matrix has been used to investigate, in bacterial photosynthetic reaction centers (RC), the coupling of long-range electron transfer to internal protein dynamics. This integral pigment-protein complex, spanning the intracytoplasmic membrane, catalyzes the primary events of photosynthetic energy transduction by promoting light-induced charge separation across the membrane dielectric (Gunner, 1991). In the RC of the purple bacterium *Rhodobacter (Rb.) sphaeroides*, absorption of a photon excites the primary electron donor, a bacteriochlorophyll dimer (P), to the first singlet state (P*). An electron is subsequently transferred (via a bacteriopheophytin, I) from P* to a first ubiquinone-10 electron acceptor (Q_A). This generates the primary charge separated state $P^+Q_A^-$ in ~200 ps. The electron is then delivered from Q_A^- to a secondary ubiquinone-10 acceptor, Q_B. In the lack of electron donors to P^+ the electron on Q_B^- recombines with the hole on P^+. In Q_B deprived RCs charge recombination occurs in the $P^+Q_A^-$ state by direct electron tunneling (Feher et al., 1989).

The low temperature kinetics of these reactions suggest that RC exists in a distribution of conformational substates, this distribution being different in the charge-separated state (i.e., in the light) as compared with the dark-adapted state (Kleinfeld et al., 1984). Feher and co-workers (Kleinfeld et al., 1984) have shown that the recombination kinetics from the primary quinone is accelerated, with respect to room temperature, when RCs are frozen to 77 K in the dark. At variance, the above process is sizably slowed down when cooling takes place under illumination; at cryogenic temperatures, in both cases, kinetics become strongly nonexponential. This behavior has been interpreted as reflecting the freezing of conformational substates, which, in turn, results in a quasi-static distribution of electron transfer rates. Such a behavior is not observed at room temperature due to the rapid substates interconversion over the time scale of the electron transfer reaction (Kleinfeld et al., 1984), which brings about averaging of free energy barriers. In a recent work (McMahon et al., 1998), it has been reported on the kinetics of $P^+Q_A^-$ recombination as a function of temperature (5–300 K), illumination protocol, and warming rate. Such a systematic study enabled the authors to characterize the relaxation processes by putting in evidence that, at high temperature, after the light-induced charge separation, the protein relaxes from a dark-adapted to a light-adapted conformation. Moreover, as suggested by Graige et al. (1998), a further conformational change is needed for transferring the electron from the primary to the secondary quinone. This change in conformation, according to x-ray data by Stowell et al. (1997), should cause an ~5 Å Q_B displacement. More recent work (Xu and Gunner, 2001) characterized a new conformational intermediate in RCs that, after having been frozen under illumination in liquid nitrogen, were rewarmed at 120 K. The above-mentioned and others, less-direct evidences (Arata and Parson, 1981; Malkin et al., 1994; Mauzerall et al., 1995; Brzezinski and Andreasson, 1995; Kalman and Maroti, 1997) indicate a close relation between electron transfer and internal protein dynamics in the RC.

In the present paper we focus on the charge recombination of the $P^+Q_A^-$ state induced by a short light-flash. We show that incorporation of the RC into dry trehalose-water matrix results, even at room temperature, in inhomogeneous kinetics similar to the ones observed at cryogenic temperatures.

MATERIALS AND METHODS

Except where otherwise stated, all chemicals were from Sigma (Darmstadt, Germany) of the highest purity and used without further purification. Trehalose was from Hayashibara Shoij Inc. (Okayama, Japan).

The RCs were isolated and purified from *Rb. sphaeroides* R-26 according to Gray et al. (1990). The secondary quinone acceptor (Q_B) was removed (≈98%) according to Okamura et al. (1975).

The concentration of trehalose in the samples is reported as percent trehalose weight fraction (wt%), i.e., (grams of trehalose/grams of trehalose plus water) %, not taking into account the contribution of RC, buffer, and detergent to the sample's weight.

Liquid samples (28% and 67% trehalose) were prepared by dissolving on aqueous buffer (5 mM Tris, pH 8.0, 0.5 mM EDTA, 0.025% lauryl dimethylamine-*N*-oxide) suitable amounts of RC; the sample composition was evaluated by weight.

Glassy samples were prepared by drying on optical glass plates of 1 × 3 cm^2 surface (Hellman) a thin layer of concentrated solution containing RC (26 μM), aqueous buffer (5 mM Tris, pH 8.0, 0.5 mM EDTA, 0.025% lauryl dimethylamine-*N*-oxide) and trehalose (0.144 g/mL). Leaving the sample under dry N_2 flow performed drying. This procedure led to a transparent, glassy sample in which the protein was incorporated. Leaving the sample under dry nitrogen atmosphere for several days produced additional drying. It was not possible to perform exhaustive drying by heating the sample at 353 K, as for trehalose-coated carboxy-myoglobin (Cordone et al., 1998, 1999); indeed, the heating at 353 K caused a dramatic increase of the pheophytin bands in the sample absorption spectrum, indicative of irreversible damages on RC. Data were collected at various times during the drying. Dry RC films were prepared by the same procedure, starting from RC solutions not containing trehalose. As the drying process proceeded, the integrity of the RC and the water content of the glasses were assayed by visible and near infrared (NIR) spectroscopy on a Lambda 19 spectrometer (Perkin-Elmer Applied Biosystems, Foster City, CA) (see Results).

The kinetics of charge recombination was measured spectrophotometrically on an apparatus of local design (Mallardi et al., 1997). To limit the exposure of the sample to the measuring light, the monitoring beam was gated shut until ~1 s before the actinic flash. During averaging cycles, samples were routinely allowed to dark adapt for more than 1 min between consecutive flash activations. For measurements in liquid samples ordinary fluorescence cuvettes were used. In the case of glasses and dry films, the plate was placed at 45° with respect to both the measuring beam and the

actinic flash; moreover, its orientation was such to avoid that the pulse reflection at the sample surface would fall on the detector. Experiments were performed at 298 K. The re-reduction of P^+, generated by a short (3-μs half-duration) Xenon flash, was monitored at 605 nm (Feher and Okamura, 1978). On selected samples, flash-induced absorption changes were recorded also at 450 nm, a wavelength that includes contributions from both P^+ and semiquinone formation on the acceptor complex (Feher and Okamura, 1978). When properly normalized, the decay kinetics recorded at the two different wavelengths were found in complete agreement.

P^+ re-reduction kinetics were fitted to a power law (see Eq. 4 in the next section) by a modified Marquardt algorithm (Bevington, 1969). Given the cross-correlation between deconvolution parameters, confidence intervals were estimated numerically by an exhaustive search method (Beechem, 1992; Holzwarth, 1996). To evaluate the error associated with the *i*th fitting parameter, a series of nonlinear minimizations was performed varying the *i*th parameter over a range of values. The other fitting parameters were allowed to adjust so as to minimize χ^2 at each value of the *i*th parameter. An error graph was obtained by plotting the minimized χ^2 versus the value of each fixed *i*th parameter. The confidence interval was obtained by using an *F*-statistic to determine the probability of a particular fractional increase in χ^2 according to

$$\chi^2/\chi^2_{\min} = 1 + [m/(n - m)]F(m, n - m, 1 - p)$$

in which m is the number of parameters, n is the number of data points, and F is the upper $(1 - p)$ quantile for Fisher's F distributions with m and $(n - m)$ degrees of freedom. Confidence intervals within two standard deviations ($p = 0.95$) calculated by this procedure are shown (see Fig. 4).

The cumulant analysis of charge recombination kinetics was previously introduced by us (Palazzo et al., 2000). The starting point is the observation of the formal correspondence between the survival probability $N(t)$ as described by Eq. 2 (in the next section) and the moment generating function $M(-t, k) \equiv \langle e^{-kt} \rangle$. The logarithm of $M(-t, k)$ is the cumulant generating function $k(-t, k) = \Sigma\, \theta_m(K)(-t)^m/m!$, in which θ_m is the mth cumulant and can be expressed as a function of the central moments μ_m of the rate distribution function $p(k)$, which characterizes $N(t)$ (see Eq. 2). In practice, the experimental kinetics have been fitted to the equation $N(t) = \exp(-\langle k \rangle t + \mu_2 t^2/2! - \mu_3 t^3/3! + (\mu_4 - 3\,\mu_2{}^2)t^4/4!)$, in which $\mu_2 \equiv \sigma^2$ is the variance of the distribution.

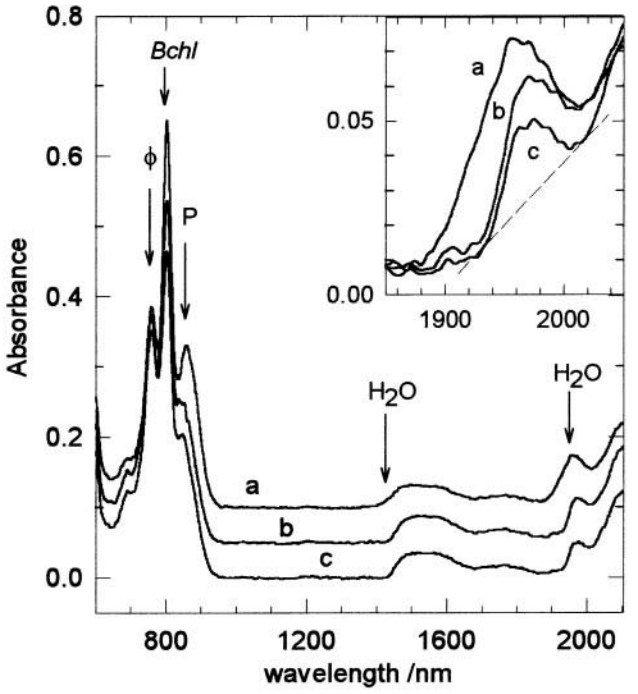

FIGURE 1 Visible-NIR absorbance spectra of an RC-containing trehalose glass at different degrees of dehydration: (*a*) after 5 h of N_2 flow (~96 wt% in trehalose); (*b*) after ~4 days storage under dry N_2 atmosphere (~97 wt% in trehalose); (*c*) after extensive dehydration (~98 wt% in trehalose). The spectra were corrected for scattering artifacts by subtracting a straight line fitted to the 1000- to 1400-nm region. For the sake of visual clarity, spectra *a* and *b* have been offset by 0.10 and 0.05 optical density units, respectively. Arrows indicate the water absorption bands and the peaks of the special pair (P), of bacteriopheophytins (ϕ) and monomer bacteriochlorophylls (*Bchl*) of the reaction center. (*Inset*) Magnification of the water combination bands; the dashed straight line is the baseline used to evaluate the area of the band for the most dry glass. Spectra shown in the inset have not been offset. The evaluation of glass composition is described in the text.

RESULTS AND DISCUSSION

Water content and RC spectral features

The evaluation of the composition of glasses at different degree of hydration is not trivial. The low amount of material and the constraint of not destroying the sample drove us to the use of NIR spectroscopy. In the NIR spectral region, water has an important combination band at ~1930 nm (due to the combination of scissoring and asymmetric stretching vibrations) and a weaker OH stretch (first overtone) at 1440 nm (Weyer, 1985).

During the course of dehydration, in parallel with measurements of $P^+Q_A{}^-$ recombination kinetics, spectra were collected in the visible-NIR region in the range 600 to 2100 nm. Three representative spectra measured in the same sample at different degrees of hydration are shown in Fig. 1. The combination band of water centered at ~1950 nm is considerably and progressively reduced upon dehydration (Fig. 1, *inset*). A decrease can be detected at 1440 nm as well. Under the most dry conditions a shift toward higher wavelengths of the combination band is also clearly observable. Such a shift is characteristic of water progressively involved in strong H-bonds (Bonner and Choi, 1974). In fact, in dilute vapor, water absorbs ~1887 nm, the absorption is shifted to 1930 nm for liquid water, and can reach 2000 nm in reverse micelles of low water content (Sunamoto et al., 1980). The area, A, delimited by the tangent to the two minima of the combination band (Fig. 1, *inset*) was used to estimate the sample water content. This is under the assumption that A is proportional to the water concentration and that the band oscillator strength is not affected by the sample hardening. A proportionality constant of 100 absorbance unit nm M^{-1} cm^{-1} inferred from water absorption in reverse micelles (Giustini et al., 1996) was used. Because the average thickness of the glass, i.e., the effective optical path, is not known and it likely depends on the water content, we use the RC absorption at 802 nm as an internal standard. This allows an estimate of the relative glass composition, when assuming that the molar ratio RC/sugar and

the extinction coefficient of the RC at 802 nm (ϵ_{802} = 288 mM^{-1} cm^{-1}) remain unchanged upon dehydration.

In all the glassy samples containing trehalose, stored at room temperature, the RC retains its spectral features and does not show any evidence of degradation for more than 2 weeks. This indicates that trehalose glass provides a "protein friendly" environment not only for small soluble proteins but also for a large integral membrane protein of high complexity, surrounded by a detergent belt. The only relevant changes upon dehydration are a blue shift and a decrease of the P long wavelength absorption maximum (at ~860 nm). Both effects are fully reversible upon increase of the water content by exposing the glasses to a water vapor atmosphere. Shifts in the Q_y band of the bacteriochlorophyll dimer are widely reported in response to changes in detergent type (Wang et al., 1994) and concentration (Gast et al., 1996) in both wild-type and mutant RCs (Farchaus et al., 1993). In general, this shift is not coupled with relevant changes in the rate of $P^+Q_A^-$ recombination. Most likely, therefore, the small changes in the RC absorption detected in dehydrated trehalose glasses have no direct physical relation with the effects observed on the kinetics of charge recombination.

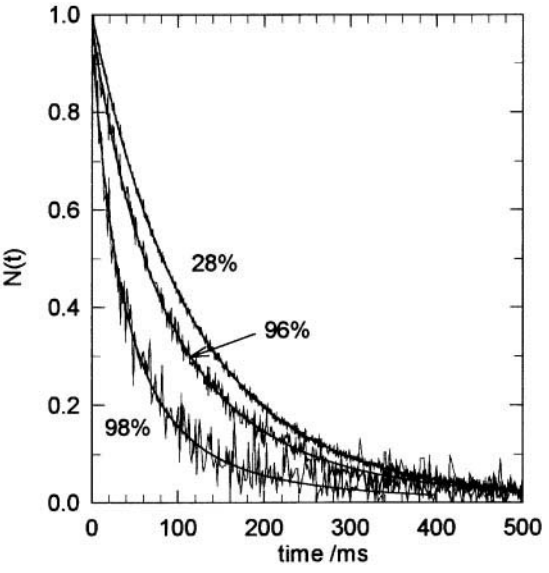

FIGURE 2 Survival probability, $N(t)$, of P^+ in 28% (wt) trehalose solution (32 averages), 96% (wt) trehalose glass (100 averages), and 98% trehalose glass (100 averages). The abscissa represents the time after the light flash. Continuous lines are the fitting according to Eq. 4.

Overview of the electron transfer kinetics and discussion of raw data

The photo-induced charge separation and the subsequent charge recombination for RCs with only the Q_A site occupied is described by

$$PQ_A \underset{k_{ap}}{\overset{h\nu}{\rightleftharpoons}} P^+Q_A^- \tag{1}$$

At room temperature the $P^+Q_A^-$ recombination is well enough described by an exponential decay, $P^+(t) = P^+(0)\, e^{-k_{AP}t}$ in which k_{AP} represents an effective rate constant resulting when both interconversion among the relevant substates and protein relaxation take place within a time window much smaller than k_{AP}^{-1}. Obviously the same exponential decay would hold true in the case that RCs would exist under a single conformation.

On the contrary, if the fluctuation among different conformational substates (characterized by individual rate constants k) is slow with respect to k_{AP}^{-1}, $N(t)$ is well described by a rate distribution $p(k)$, i.e.,:

$$N(t) = \frac{P^+(t)}{P^+(0)} = \int_0^\infty p(k) e^{-kt} dk \tag{2}$$

When the rate distribution function, $p(k)$, giving the probability that the process occurs with rate coefficients between k and $k + dk$, is not known a priori one can still determine the mean rate constant, $\langle k \rangle$, and the variance σ^2 of $p(k)$ by means of cumulant analysis of the experimental decays (Palazzo et al., 2000). Fig. 2 shows the normalized kinetics of $P^+Q_A^-$ charge recombination, measured after a single flash, in RCs suspended in a trehalose dilute solution or embedded in trehalose glasses of two different hydration levels. In solution, the electron transfer from P^+ to Q_A^- can be described by a single exponential decay with a rate constant of 8.2 s^{-1}. It must be mentioned, however, that a slightly better fit is obtained by using two exponential components with close rate constants. When RCs are embedded in trehalose glasses the overall time course of charge recombination is sped up, the mean rate constant being larger in "dry" than in "wet" glasses (Fig. 2). In addition to the acceleration of P^+ decay, incorporation of RCs in glasses leads to a markedly nonexponential behavior of the kinetics. This is better evidenced in the log-log plot shown in Fig. 3. We note that the nonexponential character of the decays increases in parallel with drying of the sample. The kinetics measured in the dehydrated glasses cannot be satisfactorily described by the sum of two exponential components, and cumulant analysis requires at least fourth order terms. No evidence exists for a specific decomposition into discrete multiple processes, whereas the smoothness and the breadth of the decays, particularly in the most dehydrated glasses (Fig. 3), strongly suggest that the kinetics reflect a continuous distribution of rate coefficients. The changes in the P^+ decay, observed upon incorporation into dry trehalose glasses, are fully reversible upon sample rehydration.

Both increase in rate and nonexponential behavior are features of the $P^+Q_A^- \rightarrow PQ_A$ electron transfer kinetics in RCs at cryogenic temperatures (Kleinfeld et al., 1984; McMahon et al., 1998).

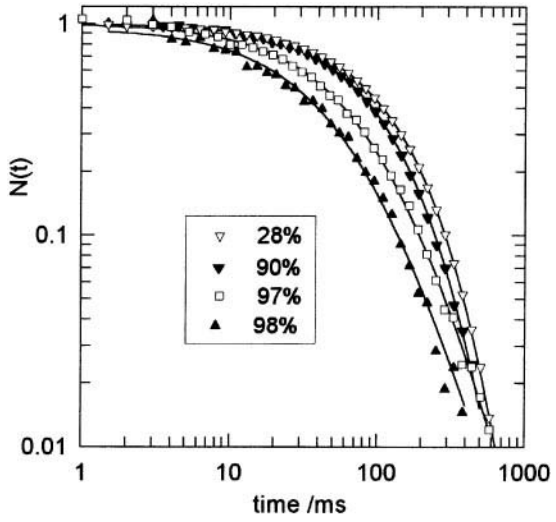

FIGURE 3 Log-log plot of P^+ decays in solution (28% wt in trehalose) and in glasses at different degree of dehydration (indicated in the label as trehalose %wt). The abscissa represents the time after the light flash. For the sake of readability, the traces, digitized in 2000 equally spaced points, have been logarithmically sampled. The whole information has been used in numerical fitting to Eq. 4 (continuous lines).

The amplitude of the flash-induced $P^+Q_A^-$ signal detected in trehalose glasses decreases progressively upon dehydration, being approximately halved in the driest sample (data not shown). The original amplitude is fully restored when the glass is rehydrated after exposure to water vapor. This effect could reflect an increased probability of recombination between P^+ and the photoreduced bacteriopheophytin I^- in the more dehydrated glasses. Interestingly, the appearance of a subnanosecond reduction phase of P^+ (not resolvable in our measurements), attributed to P^+I^- recombination, has been reported in *Rb. sphaeroides* RCs upon H_2O-D_2O isotope replacement or partial substitution of water by organic solvents (Paschenko et al., 1987).

Analysis of the electron transfer kinetics

The nonexponential charge recombination kinetics measured in trehalose glasses contain information on the rate distribution function $p(k)$ in Eq. 2. In principle $p(k)$ can be obtained by performing the inverse Laplace Transform of the experimental data set in the time domain. The inversion of the Laplace Transform is ill conditioned, and several alternative numerical methods have been proposed to overcome this problem (for a critical review see Štêpánek (1993)). In the present case, however, we preferred to use a model function and fit the data in the time domain. By considering that numerical analysis of nonexponential $P^+Q_A^-$ recombination kinetics at cryogenic temperatures yielded a unimodal $p(k)$ (McMahon et al., 1998), we chose to approximate our unknown distribution, assumed to be unimodal, by a γ-distribution, i.e.,

$$p(k) = \frac{k^{n-1}}{k_0^n} \frac{\exp\left(-\frac{k}{k_0}\right)}{\Gamma(n)} \tag{3}$$

in which $\Gamma(n)$ is the γ function. The advantage of this assumption is twofold: on the k-domain this distribution is very flexible (it can describe both symmetrical and asymmetrical unimodal distributions); on the time domain it yields a simple description of the P^+ decay, because its Laplace transform is given simply by

$$N(t) = l[p(k)] = (1 + k_0 t)^{-n} \tag{4}$$

This power law has been widely used in the analysis of ligand binding to myoglobin (Austin et al., 1975) and was found to satisfactorily account for $P^+Q_A^-$ recombination in RCs cooled at cryogenic temperatures both in the dark and in the light (Kleinfeld et al., 1984). It turned out that Eq. 4 could also accurately describe our experimental data under all the conditions (see the fits in Figs. 2 and 3). From the best fit parameters k_0 and n the first moment ($\langle k \rangle = n \cdot k_0$) and the variance ($\sigma^2 = n \cdot k_0^2$) of the γ-distribution can be evaluated and compared with those independently obtained from the model-free cumulant analysis of the kinetics (Fig. 4). The close agreement between the results of the two approaches confirms that Eq. 3 well describes the rate distribution $p(k)$ (of course cumulant analysis gives only the moments of $p(k)$ and *not* the distribution itself). Using Eq. 3, with n and k_0 values obtained from the fits to Eq. 4, we calculated $p(k)$ for all the samples. To allow an easy comparison of these distributions to those obtained from the analysis of $P^+Q_A^-$ recombination at low temperature by McMahon et al. (1998), in Fig. 5 we show our rate distribution functions, $f(k)$, defined on a logarithmic k scale (the distribution functions defined on linear and logarithmic scale are related by: $p(k)\mathrm{d}k = f(k)d\ \log(k)$).

Two features of Fig. 5 deserve some comments. The first is the remarkable agreement between the rate distributions obtained in trehalose glasses at room temperature and those obtained at cryogenic temperature in water/glycerol (compare with Fig. 1 of McMahon et al., 1998). Indeed, in the most dry trehalose glass $\langle \mathrm{Log}(k/\mathrm{s}^{-1}) \rangle = \int \mathrm{Log}(k) f(k)\ \mathrm{dLog}(k)$ is 1.3. This value compares with $\langle \mathrm{Log}(k/\mathrm{s}^{-1}) \rangle = 1.6$ for RCs cooled in the dark at 5 K (McMahon et al., 1998). The standard deviation of $f(k)$ (defined as $[\int f(k)\ (\mathrm{Log}(k) - \langle \mathrm{Log}(k) \rangle)^2 \mathrm{dLog}(k)]^{1/2}$) reveals the same agreement, being 0.32 (decades) in the room temperature dry glass and 0.2 (decades) at 5 K (McMahon et al., 1998). The second point is that already in solution, both in the presence of 0.144 g/mL trehalose (Fig. 5) and in the absence of trehalose (see caption of Fig. 6) the decay of P^+, when fitted to Eq. 4, yields a distribution of rate constants $p(k)$ of small but finite width. Nonexponential kinetics of $P^+Q_A^-$ recom-

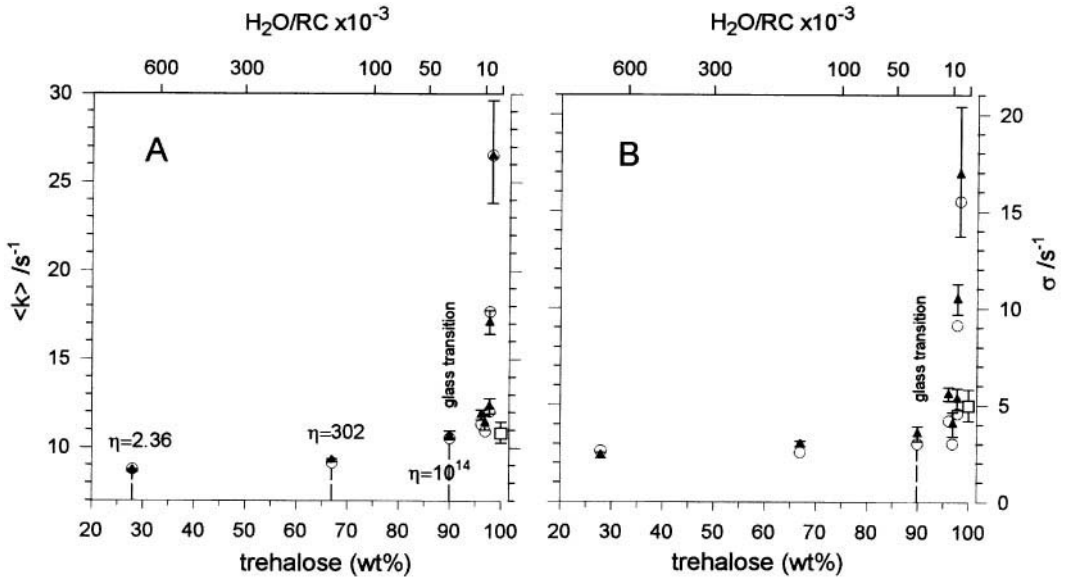

FIGURE 4 Mean ($\langle k \rangle$, *A*) and standard deviation (σ, *B*) of the rate distribution function $p(k)$ governing the $P^+Q_A^-$ recombination in trehalose solutions and glasses. Both parameters are shown as a function of the wt% of trehalose (lower scale) and of the molar ratio water/reaction center (upper scale). $\langle k \rangle$ and σ were evaluated from the experimental traces using two different methods: 1) by fitting the data to Eq. 4, i.e., assuming that $p(k)$ is a γ-distribution (see Eq. 3) (▲); 2) by fitting the data to a fourth order cumulant expansion (see Materials and Methods) (○). The vertical bars correspond to confidence intervals within 2 standard deviations evaluated numerically as described in the Materials and Methods section. In *A* the viscosity values (mPa s) of the solutions (inferred from Rampp et al., 2000) and at the glass transition (assumed to be 10^{14} mPa s (Debenedetti and Stillinger, 2001)) are reported. Both panels also show $\langle k \rangle$ and σ values determined in dry films of RCs in the absence of trehalose (□); of course for these values the only relevant abscissa is the ratio water/RC (upper scale).

bination have been observed in solution, at room temperature, in systems in which the time scale of $P^+Q_A^-$ recombination is of the order of few milliseconds. Such systems are e.g., RCs from *Rps. viridis* (Sebban and Wraight, 1989) and RCs from *Rb. sphaeroides* reconstituted with low potential quinones (Sebban, 1988; Xu and Gunner, 2000). The nonexponential kinetics have been attributed to two populations of RCs, characterized by different protonation states

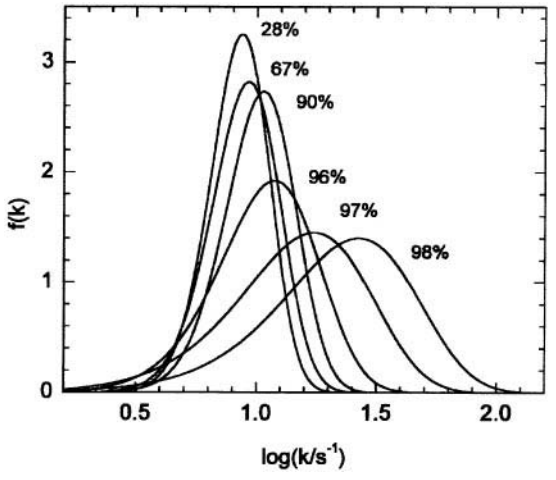

FIGURE 5 Rate distribution functions, $f(k)$, defined on a logarithmic scale, for the $P^+Q_A^-$ recombination of RC in mixtures of water and trehalose at different wt% of sugar. Samples with wt%< 90 are liquid, the other glasses. Distributions have been calculated using Eq. 3 with k_0 and n values obtained by fitting kinetic traces to Eq. 4. See text for details.

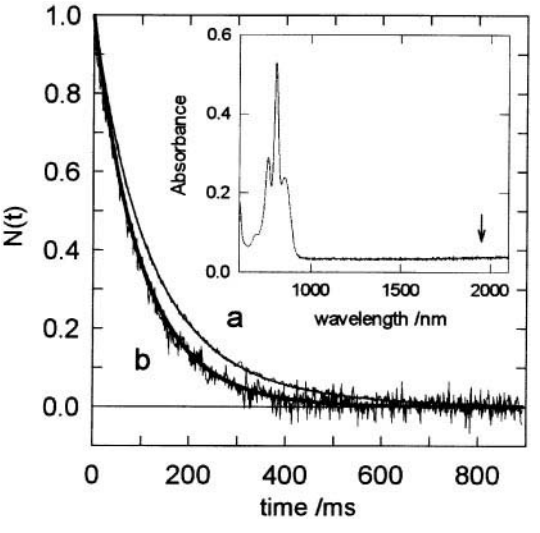

FIGURE 6 Experiments on RC dried without trehalose: normalized P^+ decays of RC in buffer (*trace a*) and in a dry film (*trace b*). Solid lines are fit to Eq. 4. From the fitting parameters k_0 and n, the following values of the mean and standard deviation σ of the rate distribution function were evaluated: $\langle k \rangle = 8.2\ s^{-1}$ and $\sigma = 2.9\ s^{-1}$ in soluton; $\langle k \rangle = 10.8\ s^{-1}$ and $\sigma = 5.0\ s^{-1}$ in the dry film. (*Inset*) Visible-NIR spectrum of a dry RC film; the position where water absorption is expected is indicated by the arrow (compare with Fig. 1).

of residues close to the Q_A binding site. For $P^+Q_A^-$ recombination occurring on a time-scale 100-fold slower (as for *Rb. sphaeroides* R-26 in solution) it is generally considered that room temperature kinetics can be adequately described by a single exponential decay, due to fluctuation averaging. As stated above, however, fitting a single exponential to the kinetics measured in solution results in small (less than 2% of the signal) but detectable nonrandom deviations. A narrow rate distribution spectrum (Fig. 5) yields a significantly improved description of the kinetics, indicating that averaging is quite effective but not complete over the time of the reaction, even in room temperature solutions.

Protein dynamics

The similarities between the kinetics we measured in trehalose glasses at room temperature and the ones observed at low temperature (McMahon et al., 1998) lead to a straightforward interpretation of our results. The generation of the charge-separated state $P^+Q_A^-$ is a substantial perturbation of the protein, inducing conformational changes, which in turn affect the subsequent electron transfer events. Several investigations give a clear evidence that after light-induced charge separation at room temperature, the protein relaxes from a dark-adapted conformation to a light-adapted conformation that can be trapped by cooling to cryogenic temperature (Kleinfeld at al., 1984; McMahon et al., 1998; Xu and Gunner, 2001). Suppression of relaxation, which normally follows charge separation at room temperature yields a faster $P^+Q_A^-$ recombination, occurring in the dark-adapted conformation of RCs. Moreover, when the interconversion among the substates, which characterize the dark-adapted state is hampered, the kinetics of $P^+Q_A^-$ recombination become strongly nonexponential.

In solution the relaxation is rapid as compared with the lifetime of $P^+Q_A^-$ and charge recombination occurs with $\langle k \rangle = 8.7\ s^{-1}$ in a protein that has adapted to the charge-separated state. At variance in extremely dry glassy samples the kinetics of $P^+Q_A^-$ recombination are characterized by an average rate constant $\langle k \rangle = 26.6\ s^{-1}$ that is three times larger than in solution. Hagen et al. (1995, 1996) reported that both substates interconversion and protein relaxation are hindered in a trehalose-coated sample of carboxy-myoglobin. This fully agrees with the findings that in a dry sample of trehalose-coated carboxy-myoglobin 1) the protein dynamics approaches the one of a harmonic system (Cordone et al., 1998; 1999), and 2) the extent of thermal interconversion among conformational A substates (Makinen et al., 1979; Vojtechovsky et al., 1999) is vanishing (Librizzi et al., 1999 and work in progress). Based on the above observations, one can interpret the continuous spectrum of rate coefficients $p(k)$ we obtain, by considering that, in our dehydrated samples, electron transfer mainly occurs in nonrelaxed proteins belonging to a inhomogeneous system in which both inhomogeneity (reflected in the parameter σ) and average rate constant $\langle k \rangle$, increase by lowering the sample water content (Figs. 4 and 5). It appears therefore that in relatively "wet" glasses interconversion between conformations and relaxation take place over a time-scale comparable with that of charge recombination. This brings about the observed $p(k)$ distribution, which results from partial averaging of the static conformational heterogeneity of RCs and is modulated by the amount of residual water. In the dry sample, trapping of conformational substates in deeper traps and the related slowing down of relaxation yields larger distributions shifted toward higher k values.

We attempt here a closer comparison between the rate distribution functions determined at cryogenic temperatures and those obtained by us in dry trehalose glasses at room temperature on the basis of the model developed by McMahon et al. (1998). These authors describe $P^+Q_A^-$ recombination in terms of quantum-mechanical nonadiabatic electron transfer theory (Fermi's golden rule and spin-boson model). In the high-temperature limit, this model reproduces the semi-classical Marcus expression for the electron transfer rates

$$k(\epsilon) = \frac{2\pi}{\hbar} V^2 \frac{1}{\sqrt{4\pi\lambda k_B T}} \exp\left[-\frac{(\epsilon - \lambda)^2}{4\lambda k_B T} \right] \qquad (5)$$

in which ϵ is the difference in energy between $P^+Q_A^-$ and PQ_A states, λ is the reorganization energy, V is the electronic interaction matrix element describing the weak coupling between the initial and final electronic states involved in electron transfer, k_B is the Boltzmann constant, and T is the absolute temperature. The authors also assume a coupling between V and ϵ of the form

$$\log V = \log V_o + \gamma(\epsilon - \epsilon_o) \qquad (6)$$

in which V_o is the value of V at the (arbitrarily chosen) energy gap ϵ_o. The heterogeneity in the RC ensemble is modeled entirely by the distribution function $g(\epsilon)$ of the energy gap between $P^+Q_A^-$ and PQ_A. The relation

$$g(\epsilon)d\epsilon = f(k)\mathrm{dlog}(k) \qquad (7)$$

correlates the energy distribution with rate distributions by means of the calculated $k(\epsilon)$ at the appropriate temperature. Using this approach, McMahon et al. (1998) concluded that in samples cooled in the dark, below 160 K, the protein is effectively frozen in the PQ_A conformation on the time scale of electron transfer and that the static heterogeneity is described by a Gaussian distribution $g(\epsilon)$.

By using Eqs. 5 through 7 with $g(\epsilon)$ and the temperature-independent parameters determined by McMahon et al. (1998), we calculated the rate distribution function $f(k)$ expected at 298 K in our driest sample by assuming that both substate interconversion and relaxation are inhibited on the time scale of the electron transfer reaction. This distribution (data not shown) is characterized by $\langle \mathrm{Log}(k/s^{-1}) \rangle = 1.33$ and standard deviation equal to 0.15 (decades). The

value obtained for $\langle \mathrm{Log}(k/s^{-1})\rangle$ is in excellent agreement with the experimentally determined one at the same temperature in the most dry trehalose glass ($\langle \mathrm{Log}(k/s^{-1})\rangle = 1.34$). A less good agreement was obtained (a factor 2) for the width of rate distribution σ whose experimental value was 0.32. These observations strongly suggest that the $f(k)$ determined in the most dry glass reflect a conformational heterogeneity of the RC not averaged on the time scale of electron transfer.

A closer inspection of the dependence of $\langle k\rangle$ and σ on sample composition (Fig. 4) reveals, however, that the influence of the glassy matrix on electron transfer kinetics is complex. Both parameters smoothly increase up to a 97% trehalose/water ratio and exhibit a sudden rise at extremely low water content. The numerical value of 97% should be taken with caution due to the approximations implicit in the evaluation of water content. However, data in Fig. 4 unambiguously show that considerable changes in the rate distribution function, reflecting the slowing of internal protein dynamics, are observed only in extremely dry samples, i.e., when the protein dynamics approaches the one of a harmonic solid (Cordone et al., 1998, 1999). At variance, the viscosity increase that must be extremely high when the trehalose/water ratio approaches 97%, only slightly affects the electron transfer process (Fig. 4).

Role of trehalose

Several observations suggest that water acts as a molecular lubricant in proteins and polypeptides (Griebenow and Klibanov, 1996; Barron et al., 1997). Below a minimal hydration level, lysozyme does not function (Careri, 1992), and several enzymes do not undergo denaturation in organic solvents (see references in Klibanov, 2001). Clayton (1978) reported that, upon dehydration of RC films, the fast phase of P^+ decay after a flash of light is accelerated and becomes temperature independent between 300 and 70 K.

To evaluate to which extent dehydration per se can contribute to the effects observed in glasses and to better understand the role of trehalose we have performed the experiments previously described also in dry films of RCs, in the absence of the disaccharide. The results can be summarized as follows. 1) In the absence of trehalose, the dehydration of samples is faster and, within our sensibility, proceeds essentially to completion. Already after 2 h of exposure to an N_2 flow a dry film is obtained. As shown in Fig. 6, no water band could be detected in the NIR spectrum of the film. 2) The reaction center spectrum exhibits the same blue shift and decrease of the P long wavelength band observed in dehydrated trehalose glasses. 3) Under these conditions, i.e., at an extremely low water content as judged from the NIR spectrum, $P^+Q_A^-$ recombination is only slightly accelerated in the dry RC film as compared with RC solutions (Figs. 4 and 6). Moreover, analysis of the kinetics in terms of a continuous spectrum of rate coefficients, yields a relatively narrow distribution function, $p(k)$. A value of σ equal to 5.0 s^{-1} was obtained in the dry film, as compared with 2.9 s^{-1} in solution and $\sigma = 16.9$ s^{-1} in extensively dehydrated trehalose glasses. It appears therefore that a substantial conformational averaging still occurs in the dry film as compared with dehydrated trehalose glasses, despite the higher water content of trehalose matrices with respect to the dry film (Fig. 4). 4) In films dried in the absence of trehalose, the photochemical activity of RCs does not withstand room temperature storage of the film longer than ~1 week. The loss of photochemical activity in the film is paralleled by a progressive increase of the pheophytin band of the RC at 760 nm (data not shown).

These results show that, under our experimental conditions, protein dehydration has almost no effect on the RC dynamics coupled to $P^+Q_A^-$ charge recombination, whereas sizable effects are observed when the protein is embedded within a glassy matrix containing trehalose and traces of residual water. This is notwithstanding the fact that the trehalose-coated sample contains more residual water than the sample dried in the absence of sugar.

The role of residual-bound water on protein function has been deeply studied by Careri and coworkers (see e.g., Careri, 1992), who showed the emergence of function (enzymatic activity for lysozyme) to coincide with the percolation threshold for proton conductivity. The extension of this concept from a small globular protein to a large membrane protein surrounded by a detergent belt is not straightforward. However, it is conceivable that patches of residual water (below the detection limit of our method) are bound to RCs dried in the absence of trehalose after 2 h of drying. This minimal hydration of the RC, in the absence of the disaccharide, could account for the essentially unaffected conformational dynamics of the RC coupled to charge recombination. In dehydrated trehalose glasses a peculiar state of the protein hydration layer is expected. A molecular dynamics study (Cottone et al., 2001) showed, in agreement with experimental results, that in a myoglobin/water/trehalose system containing 89% (w/w) trehalose/(trehalose + water) the overall mean square fluctuations of all protein atoms are sizably reduced. Moreover, the same simulation seems to suggest (work in progress) that in such system structures are formed involving a high fraction of water molecule hydrogen bonded both to the protein and to the sugar OH groups. This gives a clue to understand why, despite the larger total water content, a dramatic inhibition of protein dynamics occurs in trehalose-coated samples as compared with RC films dried in the absence of trehalose.

Our results show that trehalose also plays an important role in preserving the integrity of the RC at room temperature and allowing cycles of dehydration and rehydration of the samples. In particular, for RC embedded in trehalose glasses the level of hydration could be finely tuned both by prolonged storage under a nitrogen atmosphere at room temperature and by exposure to water vapor for different

time intervals. At variance, in the absence of trehalose, it is extremely hard to regulate the level of sample hydration.

Several studies have been, in the recent past, addressed to the study of the effects of trehalose coating on the dynamics of myoglobin. The results (Hagen et al., 1995, 1996; Cordone et al., 1998, 1999; Librizzi et al., 1999) have shown nonambiguously that the protein motional freedom is largely reduced, approaching the one of a harmonic solid for extremely dry systems. Analogous findings have also been reported by Gottfried et al. (1996) in a study on carboxyhemoglobin. Our results show that insertion into a trehalose glass sizably affects the room temperature dynamics also in a large membrane protein, screened by a detergent belt (Roth et al., 1989), as the photosynthetic RC, leading to severe hindrance of conformational dynamics when hydration drops below a critical level.

Kramer theory has provided a basis for describing unimolecular processes in condensed phases such as conformational changes in a protein. In the limit of strong friction (overdamped region) the rate constant of the interconversion, κ, is given by (Billing and Mikkelsen, 1996):

$$\kappa = \frac{A}{\zeta}\exp\left(-\frac{E_0}{k_B T}\right) \tag{8}$$

in which k_B is the Boltzmann's constant, E_0 is the average height of the potential energy barrier separating protein substates, A is a T-independent parameter depending only on the shape of the potential surface. In Eq. 8 the single friction constant (ζ) fixes the strength of the interaction between the reaction coordinate and the remaining degrees of freedom. In some cases the interpretation of ζ is straightforward: for myoglobin in several solvents ζ has been essentially identified with the bulk viscosity η of the medium (Ansari et al., 1992). Therefore, Eq. 8 enabled to rationalize, at molecular level, the effect of the environment and to conclude that the surface diffusive motions are strongly coupled with the reactive modes of the protein, the former being slowed down by a mere solvent viscosity effect.

Fig. 4 evidences that the dynamics of RCs in a trehalose matrix is not simply related to viscosity. Indeed, at trehalose/water ratios $\approx$90%, i.e., under conditions in which a trehalose water system is in a glassy state (Green and Angell, 1989), no dramatic viscosity effects are detected on the kinetics of $P^+Q_A^-$ recombination, notwithstanding the extremely large bulk viscosity increase at the glass transition.

The relevance of parameters, other than viscosity as the elastic modulus and the compressibility of the environment, in determining internal protein dynamics has been recently suggested by an infrared vibrational echo study performed in myoglobin (Rector et al., 2001). These authors reported that protein structural fluctuations involving displacements of the protein surface can take place even in highly viscous fluids but are severely hindered when a solid external matrix fixes the protein surface topology. Accordingly, one expects the sizable decrease in protein volume that accompanies the formation of the charge separated state in RC (Edens et al., 2000) be severely hindered when the trehalose-water matrix approaches the dynamic behavior of a harmonic solid (Cordone et al., 1998, 1999; Cottone et al., 2001). In turn, the internal dynamics of the protein, on the time scale of the electron transfer reaction examined, also is expected to be constrained.

The above reported arguments enable us to rationalize the behavior of the rate constants distributions reported in Fig. 5. Indeed, for trehalose concentration $<$90% the (nonsolid) external matrix affects the internal protein dynamics by a mere viscosity effect. Under such condition, substates interconversion, although slowed down, can take place. Accordingly, both averaging of free-energy barriers and protein relaxation, whose rates decrease with increasing viscosity, can take place. As Fig. 5 shows, the above rate decrease brings about 1) slight displacements toward higher rates of electron transfer due to the slowing down of the relaxation process and 2) slight broadening of the distributions due to the lower rate of averaging of free energy barriers.

For trehalose concentration $>$90%, the matrix behaves as a solid glass. This can be inferred from the phase diagram of the water/trehalose system (Green and Angell, 1989; Conrad and de Pablo, 1999). In this concentration range, the distribution in Fig. 5 exhibits dramatic variations similar to the ones observed at cryogenic temperature (McMahon et al., 1998). As mentioned above, in a solid trehalose matrix, the internal dynamics of a protein approach the one of a harmonic solid in which no interconversion among conformational substates and protein relaxation can take place. Accordingly, as shown in Fig. 5 one has 1) a sizable broadening of the distributions due to the fact that the free energy barriers have become quasi static and 2) a displacement toward higher rates of electron transfer due to lack of protein relaxation. As evident from Fig. 5, both of the above effects increase with trehalose concentration, i.e., with increasing matrix rigidity.

CONCLUSIONS

The reported results indicate that embedding RCs in a trehalose matrix strongly affects protein internal motions coupled to long-range electron transfer. Indeed, the thermal fluctuations among conformational substates are progressively (but slightly) hindered with increasing "solvent" viscosity, up to trehalose concentration $\sim$90%. For larger sugar concentrations, the matrix increasingly approaches a solid glass, thus causing the observed hindering of substates interconversion. This results in a broad distribution of rate constants for electron transfer. Dehydration of trehalose-coated samples inhibits in a parallel way the relaxation from

dark-adapted to light-adapted conformation, which follows primary charge separation at room temperature. This brings about displacements toward larger rates of electron transfer that become particularly large for sugar concentrations at which the matrix is a solid glass. Interesting information is obtained by comparing the inhomogeneous recombination kinetics we observed at room temperature in extensively dried water-trehalose glasses with those measured in glycerol-water mixtures at cryogenic temperatures (McMahon et al., 1998). Such a comparison confirms that, in the dehydrated solid matrix, both interconversion among substates and relaxation are essentially blocked, over the time-scale of $P^+Q_A^-$ charge recombination (i.e., hundreds of milliseconds). Analogous effects increasing with the sugar/water ratio have been detected for the internal dynamics of trehalose-coated carboxy-myoglobin (Librizzi et al., 1999 and work in progress).

The driest trehalose-coated samples we studied contain larger amount of residual water than the sample dried in the absence of sugar; this notwithstanding, the dynamics of the latter sample is barely affected by the lack of water, whereas the dynamics of the former is extremely hampered. The comparison between the dynamic behaviors of samples respectively dried in the presence and in the absence of sugar puts forward the relevance of residual water in blocking trehalose coated RCs in suitable, nondamaged conformations.

The function-dynamics coupling in protein is usually studied by analyzing the functional behavior in wide temperature intervals, spanning from cryogenic to room temperature (Austin et al., 1975; Hagen et al., 1996; McMahon et al., 1998). This enables us to study the functional behavior under conditions in which protein dynamics approaches the harmonic behavior, thus hampering substates interconversion and protein relaxation. However, under such conditions the motional thermal energy of the "harmonic" protein is not the room temperature one, i.e., the one at which the protein function takes place. At variance, the measurements reported in this paper have the advantage of studying electron transfer in the RC, when the protein dynamics approaches the one of a harmonic solid at constant (room) temperature.

We think of particular relevance is the fact that the functional behavior of a RC sample under six different solvent conditions and exhibiting six different "dynamic" behaviors at room temperature (Fig. 5) can be coherently rationalized within the framework of an extremely simple model. This gave insights on the function-dynamics coupling at room temperature in the reaction center.

We thank B. A. Melandri, P. Turina, M. Giustini, G. Cottone, F. Librizzi, and E. Vitrano for extremely useful discussions.

This work is part of a Project co-financed by the Italian Ministry for University and Scientific and Technological Research (MURST) and by the European Community (European Funds for Regional Development). The financial support of MURST, grant PRIN/99, Bioenergetica e Trasporto di Membrana, is acknowledged by G.V. G.P. was supported by Consorzio Interuniversitario dei Sistemi a Grande Interfase (CSGI-Firenze).

REFERENCES

Ansari, A., C. M. Jones, E. R. Henry, J. Hofrichter, and W. A. Eaton. 1992. The role of solvent viscosity in the dynamics of protein conformational changes. *Science.* 256:1796–1798.

Arata, H., and W. W. Parson. 1981. Enthalpy and volume changes accompanying electron transfer from P-870 to quinones in *Rhodopseudomonas sphaeroides* reaction centers. *Biochim. Biophys. Acta.* 636:70–81.

Austin, R. H., K. W. Beeson, L. Eisenstein, H. Frauenfelder, and I. C. Gunsalus. 1975. Dynamics of ligand binding to myoglobin. *Biochemistry.* 14:5355–5373.

Barron, L. D., L. Hecht, and G. Wilson. 1997. The lubricant of life: a proposal that solvent water promotes extremely fast conformational fluctuations in mobile heteropolypeptide structure. *Biochemistry.* 36: 13143–13147.

Beechem, J. M. 1992. Global analysis of biochemical and biophysical data. *Methods Enzymol.* 20:37–54.

Bevington, P. R. 1969. Data Reduction and Error Analysis for the Physical Sciences. McGraw-Hill, New York.

Billing, G. D., and K. V. Mikkelsen. 1996. Energetic aspects of solvent effects on solutes. *In* Introduction to Molecular Dynamics and Chemical Kinetics. John Wiley and Sons, Inc, New York. 98–163.

Bonner, O. D., and Y. S. Choi. 1974. Hydrogen bonding of water in organic solvent. *J. Phys. Chem.* 78:1723–1731.

Brzezinski, P., and L.-E. Andreasson. 1995. Trypsin treatment of reaction centers from *Rhodobacter sphaeroides* in the dark and under illumination: protein structural changes follow charge separation. *Biochemistry.* 34:7498–7506.

Careri, G. 1992. Proton percolation and emergence of function in nearly dry biosystems *Nanobiology.* 1:117–126.

Clayton, R. K. 1978. Effects of dehydration on reaction centers from *Rhodopseudomonas sphaeroides. Biochim. Biophys. Acta.* 504:255–264.

Conrad, P. B., and J. J. de Pablo. 1999. Computer simulations of the cryoprotectant disaccharide α, α-trehalose in aqueous solution. *J. Phys. Chem. A.* 103:4049–4045.

Cordone, L., M. Ferrand, E. Vitrano, and G. Zaccai. 1999. Harmonic behavior of trehalose-coated carbon-monoxy-myoglobin at high temperature. *Biophys. J.* 76:1043–1047.

Cordone, L., P. Galajada, E. Vitrano, A. Gassmann, A. Ostermann, and F. Parak. 1998. A reduction of protein specific motions in co-ligated myoglobin embedded in a trehalose glass. *Eur. Biophys. J.* 27:173–176.

Cottone, G., L. Cordone, and G. Ciccotti. 2001. Molecular dynamics simulation of carboxy-myoglobin embedded in a trehalose-water matrix. *Biophys. J.* 80:931–938.

Crowe, L. M., D. S. Reid, and J. H. Crowe. 1996. Is trehalose special for preserving dry biomaterials? *Biophys. J.* 71:2087–2093.

Debenedetti, P. G., and F. H. Stillinger. 2001. Supercooled liquids and the glass transition. *Nature.* 410:259–267.

Edens, G. J., M. R. Gunner, Q. Xu, and D. Mauzerall. 2000. The enthalpy and entropy of reaction for formation of $P^+Q_A^-$ from excited reaction centers of *Rhodobacter sphaeroides. J. Am. Chem. Soc.* 122:1479–1485.

Farchaus, J. W., J. Wachtveitl, P. Mathis, and D. Oesterhelt. 1993. Tyrosine 162 of the photosynthetic reaction center L-subunit plays a critical role in the cytochrome c_2 mediated rereduction of the photooxidized bacteriochlorophyll dimer in *Rhodobacter sphaeroides*: I. Site-directed mutagenesis and initial characterization. *Biochemistry.* 32: 10885–10893.

Feher, G., J. P. Allen, M. Y. Okamura, and D. C. Rees. 1989. Structure and function of bacterial photosynthetic reaction centres. *Nature.* 33: 111–116.

Feher, G., and M. Y. Okamura. 1978. Chemical composition and properties of reaction centers. *In* The Photosynthetic Bacteria. R. K. Clayton and W. R. Sistrom, editors. Plenum Press, New York. 349–386.

Frauenfelder, H., and B. McMahon. 1998. Dynamics and function of proteins: the search for general concepts. *Proc. Natl. Acad. Sci. U.S.A.* 95:4795–4797.

Frauenfelder, H., F. Parak, and R. D. Young. 1988. Conformational substates in proteins. *Annu. Rev. Biophys. Biophys. Chem.* 17:451–479.

Frauenfelder, H., S. G. Sligar, and P. G. Wolynes. 1991. The energy landscapes and motions of proteins. *Science.* 254:1598–1603.

Frauenfelder, H., and P. G. Wolynes. 1994. Biomolecules: where the physics of complexity and simplicity meet. *Phys. Today.* 47:58–64.

Gast, P., P. W. Hemelrijk, H. J. Van Gorkom, and A. J. Hoff. 1996. The association of different detergents with the photosynthetic reaction center protein of *Rhodobacter sphaeroides* R26 and the effects on its photochemistry. *Eur. J. Biochem.* 239:805–809.

Giustini, M., G. Palazzo, G. Colafemmina, M. Della Monica, M. Giomini, and A. Ceglie. 1996. Microstructure and dynamics of the water-in-oil CTAB/*n*-pentanol/*n*-hexane/water microemulsion: a spectroscopic and conductivity study. *J. Phys. Chem.* 100:3190–3198.

Gottfried, D. S., E. S. Peterson, A. G. Sheikh, J. Wang, M. Yang, and J. M. Friedman. 1996. Evidence for damped hemoglobin dynamics in a room temperature trehalose glass. *J. Phys. Chem.* 100:12034–12042.

Graige, M. S., G. Feher, and M. Y. Okamura. 1998. Conformational gating of the electron transfer reaction $Q_A^{-}Q_B$ 224 $Q_AQ_B^{-}$ in bacterial reaction centers of *Rhodobacter sphaeroides* determined by a driving force assay. *Proc. Natl. Acad. Sci. U.S.A.* 95:11679–11684.

Gray, K. A., J. W. Farchaus, J. Wachtveitl, J. Breton, and D. Oesterhelt. 1990. Initial characterization of site-directed mutants of tyrosine M210 in the reaction centre of *Rhodobacter sphaeroides*. *EMBO J.* 9:2061–2070.

Green, J. L., and C. A. Angell. 1989. Phase relations and vitrification in saccharide-water solutions and trehalose anomaly. *J. Phys. Chem.* 93: 2880–2882.

Griebenow, K., and A. M. Klibanov. 1996. On protein denaturation in aqueous-organic mixtures but not in pure organic solvents. *J. Am. Chem. Soc.* 47:11695–11700.

Gunner, M. R. 1991. The reaction center protein from purple bacteria: structure and function. *Curr. Topics Bioenerg.* 16:319–367.

Hagen, S. J., J. Hofrichter, and W. A. Eaton. 1995. Protein reaction kinetics in a room-temperature glass. *Science.* 269:959–962.

Hagen, S. J., J. Hofrichter, and W. A. Eaton. 1996. Geminate rebinding and conformational dynamics of myoglobin embedded in a glass at room temperature. *J. Phys. Chem.* 100:12008–12021.

Holzwarth, A. R. 1996. Data analysis of time-resolved measurements. *In* Biophysical Techniques in Photosynthesis. J. Amesz and A. J. Hoff, editors. Kluwer Academic Publishers, Dordrecht, The Netherlands. 75–92.

Kalman, L., and P. Maroti. 1997. Conformation-activated protonation in reaction centers of the photosynthetic bacterium *Rhodobacter sphaeroides. Biochemistry.* 36:15269–15276.

Kleinfeld, D., M. Y. Okamura, and G. Feher. 1984. Electron transfer kinetics in photosynthetic reaction centers cooled to cryogenic temperatures in the charge-separated state: evidence for light-induced structural changes. *Biochemistry.* 23:5780–5786.

Klibanov, A. M. 2001. Improving enzymes by using them in organic solvents. *Nature.* 409:241–246.

Leslie, S. B., E. Israeli, B. Lighthaert, J. H. Crowe, and L. M. Crowe. 1995. Trehalose and sucrose protect both membranes and proteins in intact bacteria during drying. *Appl. Environ. Microbiol.* 91:3592–3597.

Librizzi, F., E. Vitrano, and L. Cordone. 1999. Inhibition of A substates interconversion in trehalose coated carbonmonoxy-myoglobin. *In* Biological Physics. H. Frauenfelder, G. Hummer, and R. Garcia, editors. AIP, American Institute of Physics, Melville, New York.132–138.

Makinen, M. W., R. A. Houtchens, and W. S. Caughey. 1979. Structure of carboxymyoglobin in crystals and in solutions. *Proc. Natl. Acad. Sci. U.S.A.* 76:6042–6046.

Malkin, S., M. S. Churio, S. Shochat, and S. E. Braslavsky. 1994. *J. Photochem. Photobiol.* B. 23:79–85.

Mallardi, A., G. Palazzo, and G. Venturoli. 1997. Binding of ubiquinone to photosynthetic reaction centers: determination of enthalpy and entropy changes in reverse micelles. *J. Phys. Chem. B.* 101:7850–7857.

Mauzerall, D. C., M. R. Gunner, and J. W. Zhang. 1995. Volume contraction on photoexcitation of the reaction center from *Rhodobacter sphaeroides* R-26: internal probe of dielectrics. *Biophys. J.* 68:275–280.

McMahon, B. H., J. D. Müller, C. A. Wraight, and G. U. Nienhaus. 1998. Electron transfer and protein dynamics in the photosynthetic reaction center. *Biophys. J.* 74:2567–2587.

Okamura, M. Y., R. A. Isaacson, and G. Feher. 1975. Primary acceptor in bacterial photosynthesis: obligatory role for ubiquinone in photoactive reaction centers of *Rhodopseudomonas sphaeroides. Proc. Natl. Acad. Sci. U.S.A.* 72:3491–3495.

Palazzo, G., A. Mallardi, M. Giustini, D. Berti, and G. Venturoli. 2000. Cumulant analysis of charge recombination kinetics in bacterial reaction centers reconstituted into lipid vesicles. *Biophys. J.* 79:1171–1179.

Paschenko, V. Z., B. N. Korvatovsky, S. L. Logunov, A. A. Kononenko, P. P. Knox, N. I. Zakharova, N. P. Grishanova, and A. B. Rubin. 1987. Modification of protein hydrogen bonds influences the efficiency of picosecond electron transfer in bacterial photosynthetic reaction centers. *FEBS Lett.* 214:28–34.

Rampp, M., C. Buttersck, and H. D. Lüdermann. 2000. c,T-dependence of the viscosity and the self-diffusion coefficients in some aqueous carbohydrate solutions. *Carbohydr. Res.* 328:561–572.

Rector, K. D., J. Jiang, M. A. Berg, and M. D. Fayer. 2001. Effects of solvent viscosity on protein dynamics: infrared vibrational echo experiments and theory. *J. Phys. Chem. B.* 105:1081–1092.

Roth, M., A. Lewit-Bentley, H. Michel, J. Deisenhofer, R. Huber, and D. Oesterhelt. 1989. Detergent structure in crystals of a bacterial photosynthetic reaction centre. *Nature.* 340:659–662.

Sebban, P. 1988. pH effect on the biphasicity of the $P^{+}Q_A^{-}$ charge recombination kinetics in the reaction centers from *Rhodobacter sphaeroides* reconstituted with antraquinones. *Biochim. Biophys. Acta.* 936: 124–132.

Sebban, P., and C. A. Wraight. 1989. Heterogeneity of the $P^{+}Q_A^{-}$ recombination kinetics in reaction centers from *Rhodopseudomonas viridis*: the effects of pH and temperature. *Biochim. Biophys. Acta.* 974:54–65.

Štêpánek, P. 1993. Data analysis in dynamic light scattering. *In* Dynamic Light Scattering. The Method and Some Applications. W. Brown, editor. Clarendon Press, Oxford. 177–241.

Stowell, M. H. B., T. M. McPhillips, D. C. Rees, S. M. Soltis, E. Abresch, and G. Feher. 1997. Light-induced structural changes in photosynthetic reaction center: implication for mechanism of electron-proton transfer. *Science.* 276:812–816.

Sunamoto, J., T. Hamada, T. Seto, and S. Yamamoto. 1980. Microscopic evaluation of surfactant-water interaction in apolar media. *Bull. Chem. Soc. Jpn.* 53:583–589.

Uritani, M., M. Takai, and K. Yoshinaga. 1995. Protective effect of disaccharides on restriction endonucleases during drying under vacuum. *J. Biochem.* 117:774–779.

Vojtechovsky, J., K. Chu, J. Berendzen, R. M. Sweet, and I. Schlichting. 1999. Crystal structures of myoglobin-ligand complexes at near-atomic resolution. *Biophys. J.* 77:2153–2174.

Wang, S., S. Lin, X. Lin, N. W. Woodbury, and J. P. Allen. 1994. Comparative study of reaction centers from purple photosynthetic bacteria: isolation and optical spectroscopy. *Photosynth. Res.* 42: 203–215.

Weyer, L. G. 1985. Near-infrared spectroscopy of organic substances. *Appl. Spectrosc. Rev.* 21:1–43.

Xu, Q., and M. R. Gunner. 2000. Temperature dependence of the free energy, enthalpy, and entropy of $P^{+}Q_A^{-}$ charge recombination in *Rhodobacter sphaeroides* R-26 reaction centers. *J. Phys. Chem. B.* 104:8035–8043.

Xu, Q., and M. R. Gunner. 2001. Trapping conformational intermediate states in the reaction center protein from photosynthetic bacteria. *Biochemistry.* 40:3232–3241.